Design, Synthesis and Anti Flaviviridae Activity of N^6-, 5′,3′-*O*- and 5′,2′-*O*-Substituted Adenine Nucleoside Analogs

Angela Angusti,[a] Stefano Manfredini,*[,a] Elisa Durini,[a] Nunzia Ciliberti,[a] Silvia Vertuani,[a] Nicola Solaroli,[a,b] Sabrina Pricl,[c] Marco Ferrone,[c] Maurizio Fermeglia,[c] Roberta Loddo,[d] Barbara Secci,[d] Anna Visioli,[d] Tiziana Sanna,[d] Gabriella Collu,[d] Margherita Pezzullo,[d] and Paolo La Colla[d]

[a] *Department of Pharmaceutical Sciences, University of Ferrara; via Fossato di Mortara 19, 44100 Ferrara, Italy:* [b] *Division of Metabolic Diseases, Karolinska University Hospital; S-141 86 Huddinge/Stockholm, Sweden:* [c] *Molecular Simulation (MOSE) Laboratory, Department of Chemical Engineering, University of Trieste; Piazzale Europa 1, 34127 Trieste, Italy: and* [d] *Department of Biomedical Sciences and Technologies, University of Cagliari; Cittadella Universitaria, 09042, Monserrato, Cagliari, Italy.*

Received August 21, 2007; accepted January 4, 2008; published online February 1, 2008

During a random screening of representative libraries of nucleoside analogues we discovered that the adenine derivatives FEVB28 and FEG118 were Flaviviridae inhibitors endowed with potency comparable, if not superior, to that of ribavirin. Those studies prompted us to design a new class of protected nucleoside analogs, reported herein, which displays interesting anti-bovine viral diarrhea virus (BVDV) activity and low cytotoxicity in cell-based assays (4, 23, 29 EC_{50}: 14, 11, 26 μM respectively, CC_{50}>100 μM) and appreciable activity in enzyme assays against the RNA dependent RNA polymerase (RdRp) of BVDV (4, 23, 29, RdRp inhibition activity 27, 16, 15 μM respectively). A molecular modeling study was also carried out to highlight the possible interactions between this compounds class and the corresponding hepatitis C virus (HCV) enzyme.

Key words adenine nucleoside analog; bovine viral diarrhea virus; RNA dependent RNA polymerase

The Flaviviridae virus family presents linear, plus sense, single-stranded RNA genome of 9.6 to 12.3-kilobases in length and is responsible for about seventy diseases, of which thirteen in humans. The viruses belonging to this family, are divided in three different genera, showing a great similarity in virion morphology, genome organization and replication strategy:[1] *Hepacivirus* [Hepatitis C Virus (HCV)], *Flavivirus* [*e.g.* Yellow Fever Virus (YFV), Dengue Fever Virus (DFV), West Nile Virus (WNV)], and *Pestivirus* [Bovine Viral Diarrhea Virus (BVDV), Border Disease Virus (BDV)].[2—5]

Bovine viral diarrhea virus (BVDV), the prototype representative of the *Pestivirus* genus, is ubiquitous and causes a range of clinical manifestations, including abortion, teratogenesis, respiratory problems, chronic wasting syndrome, immune system dysfunction, and predisposition to secondary viral and bacterial infections.[5]

Regardless of the availability of vaccines[6] against BVDV and the increasingly elaborate eradication or control of programs, BVDV continues to be a financial burden to the farming industry. An alternative approach against BVDV infections could be the use of antiviral agents that specifically inhibit the replication of the virus. Although not suited to treat large herds, it could be important to have selective anti-*Pestivirus* compounds on hand.

Recently, a number of selective anti-BVDV compounds have been reported. These include the following: polymerase inhibitors *i.e.* *N*-propyl-*N*-[2-(2*H*-1,2,4-triazino[5,6-*b*]indol-3-ylthio)ethyl]-1-propanamine (VP32947),[7] a thiazole urea derivative,[8] a cyclic urea derivative[9] and inhibitors of the NS3/NS4A protease, for example, a boron-modified peptidyl mimetic.[10] Aromatic cationic molecules have also been reported to inhibit BVDV replication, although the mechanism of action remains to be elucidated.[11] Other BVDV inhibitors target cellular enzymes such as the α-glucosidase[12—14] and inosine monophosphate dehydrogenase (IMPDH).[15] Recently, a new highly selective BVDV polymerase inhibitor of pestivirus replication, 5-[(4-bromophenyl)methyl]-2-phenyl-5*H*-imidazo[4,5-*c*]pyridine (BPIP), was reported.[16]

Like BVDV, HCV also belongs to the Flaviviridae family. It is an important cause of chronic hepatitis throughout the world and is the most common factor involved in the development of liver cirrhosis and hepatocellular carcinoma.[17,18] The licensed therapy based on the combination of pegylated interferon-α with the broad spectrum antiviral agent ribavirin, has a limited efficacy (about 60%) and there are important side effects associated with the therapy. Therefore, highly effective and selective inhibitors of HCV replication are urgently required.[19]

BVDV is considered to be a valuable surrogate virus model for identifying and characterizing antiviral agents for use against HCV.[20] In some aspects of viral replication, BVDV is more advantageous than the currently used HCV replicon systems[21,22] because this latter does not present a complete replication cycle thus excluding from the study some viral stages of viral replication. Therefore, insight into the mechanism of antiviral activity of anti-*pestivirus* compounds may provide valuable information for the design of novel antiviral strategies against HCV.

In the course of a screening effort dedicated to the search for new classes of inhibitors of BVDV, two adenine analogues FEVB28[23] and FEG118[24] (Fig. 1) were found to elicit Flaviviridae[25] activity in the micromolar range comparable to those of Ribavirin (Table 1).

The shift of the BVDV activity from 10 μM (in the FEVB28) to >100 μM (in the araA), suggested that the cleavage of silyl groups of compound FEVB28, led to loss of antiviral activity. The same phenomenon does not occur with

* To whom correspondence should be addressed. e-mail: s.manfredini@unife

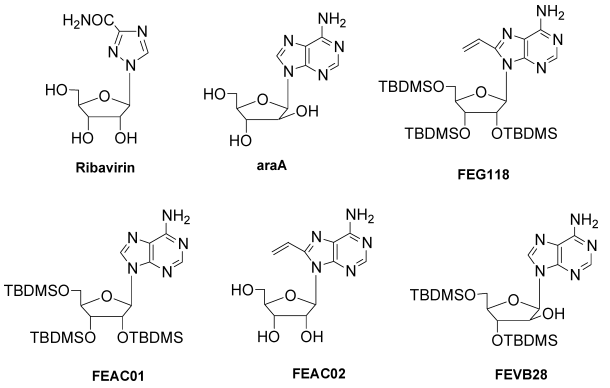

Fig. 1. Structure of Ribavirin, araA, FEG118, FEVB28, FEAC01[27] and FEAC02[26]

Table 1. Cytotoxicity and Antiviral Activity of FEVB28 and FEG118 and Congeners, Compared to Ribavirin and araA

Compounds	MDBK CC_{50} *a)*	BHK-21 CC_{50} *a)*	BVDV EC_{50} *b)*	YFV EC_{50} *b)*	DFV-2 EC_{50} *b)*	WNV EC_{50} *b)*
Ribavirin	>100	>100	30	30	ND	ND
FEVB28	>100	>100	10	70	>100	>100
FEG118	>100	15	20	7.5	7.5	>15
araA	>100	90	>100	>90	>90	>90
FEAC02	5	14	>5	>14	>14	>14
FEAC01	14	5	>14	>5	>5	>5

a) Compound concentration (μM) required to reduce the viability of mock-infected cells by 50%, as determined by the MTT or plaque reduction method. *b*) Compound concentration (μM) required to achieve 50% protection from virus-induced cytopathogenicity, as determined by the MTT method. ND: Not Detected

FEG118. In fact, its desilylated counterpart (FEAC02[24]) is cytotoxic at concentrations as low as 5—14 μM, which are lower than the FEG118 concentration active against BVDV (20 μM). Interestingly, FEG118 is active also against YFV, and DFV-2.

Moreover, it was impossible to ascertain the relevance of the vinyl group in the antiviral activity of FEG118. In fact, its unsubstituted counterpart (FEAC01,[26] Fig. 1) is also highly cytotoxic (5—14 μM) (Table 1).

We could therefore conclude that, in adenine derivatives endowed with low cytotoxicity, the anti-BVDV activity correlates with: i) the presence of both silyl groups and a vinyl substituent at C-8 position in *ribo* nucleosides, and ii) the presence of silyl groups in *ara* nucleosides.

In view of this important result, and the lack of effective antiviral agents against the Flaviviridae family, we decided to investigate thoroughly compounds FEG118 and FEVB28. In particular, the first phase of the project took into consideration FEVB28 as a template for a new generation of compounds, modified at the sugar portion by introduction of different substituents.

Concomitantly, preliminary molecular modeling investigations, enzymatic assays, and *in vitro* antiviral activity have been carried out to identify the possible target. In particular, in view of the nucleoside nature of the compounds, our attention was directed towards the NS5B. The non structural protein 5B (NS5B) is an RNA-dependent RNA polymerase (RdRp) which plays a central role as a catalytic enzyme in viral replication.

Chemistry Starting from the general structure of lead

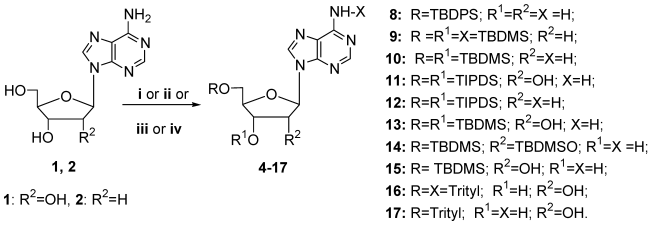

(i) Pyridine, TBDPSCl or TBDMSCl, r.t.; (ii) DMF, TBDPSCl or TBDMSCl, imidazole or TEA, r.t. or 70 °C; (iii) $TIPDSCl_2$, pyridine, reflux; (iv) pyridine, trityl-Cl, 60 °C.

Chart 1

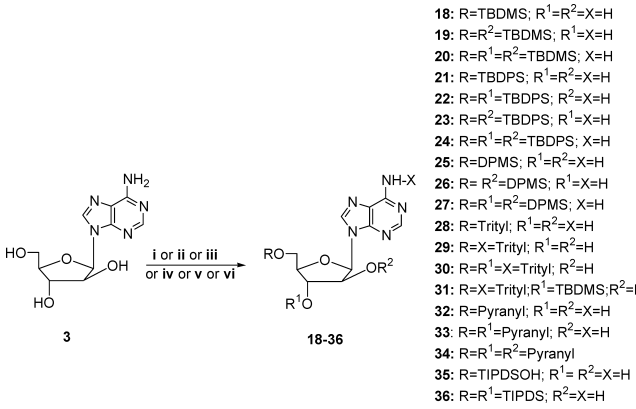

(i) Pyridine, TBDMSCl or TBDPSCl or DPMSCl, r.t.; (ii) DMF, TBDMSCl or TBDPSCl or DPMSCl, imidazole, r.t.; (iii) DMF, TBDMSCl, TEA, 60 °C; (iv) pyridine, trityl-Cl or trityl-Br, r.t. to 105 °C ; (v) DMF, *p*-TsOH, DHP; (vi) pyridine, $TIPDSCl_2$, reflux.

Chart 2

compounds we investigated ribo-, 2′-deoxyribo- and arabinofuranosyl derivatives of adenine. Based on simple rational concepts (*i.e.* different bulk and nature of the bonding groups) and synthetic availability, different substituents were introduced at the hydroxyl functions. In particular, *tert*-butyldimethylsilyl (TBDMS), methyldiphenylsilyl (DPMS), *tert*-butyldiphenylsilyl (TBDPS), tetraisopropyldisiloxyl (TIPDS), pyranyl and triphenylmethyl groups were considered. TBDPS, TBDMS, DPMS derivatives were prepared following the synthetic procedure described by Ogilvie *et al*.[27,28] In particular 5′-*O*-silyl derivatives were obtained by treatment with the silylating agent in pyridine at room temperature (**4**,[29] **8**, **15**,[30] **18**, **21**,[29] **25**) (Charts 1, 2).

The preparation of the more hindered 2′,5′- and 3′,5′-bis-*O*-silylated derivatives (TBDPS, DPMS) required an excess of silylating agent, imidazole or triethylamine (TEA), dimethylformamide (DMF) as solvent (**5**, **6**, **7**, **9**, **10**,[31] **13**,[32] **14**,[32] **22**, **23**, **26**) and in some cases gentle heating to improve the yield (70 °C, compounds **5** and **6**). Traces of persilylated derivatives (compounds **24**, **27**) were also isolated from the reaction mixture during the synthesis of compounds **23** and **26**. Differently, the preparation of 2′,5′-bis-*O*-TBDMS araA (**19**[33]) required the presence of *tert*-butyldimethylsilyl chloride (TBDMSCl) and $AgNO_3$ as catalyst. Fully silylated TBDMS derivative **20** was obtained according to the known synthetic methodology[34] (Chart 2).

TIPDS derivatives (**11**,[35] **12**,[36] **36**[37]) were obtained apply-

ing the synthetic strategy reported by Robins *et al.*[38] (Charts 1, 2). In the case of araA the product of incomplete cyclization at the 3′-OH (**35**) was also isolated.

Preparation of trityl derivatives of adenosine and araA (**16**,[39] **17**,[40] **28**, **29**, **30**), was carried out adapting previously described procedures.[41,42] Moreover, to combine different kinds of substituents, compound **29** was further modified by introduction of a TBDMS group on 3′-OH (**31**), this was achieved under standard conditions (imidazole, DMF, room temperature). The preparation of the pyranyl derivatives of araA (**32**, **33**, **34**) was carried out following and adapting a known synthetic procedure[43] (Chart 2).

Biology Cytotoxicity: Cytotoxicity was evaluated in exponentially growing human $CD4^+$ lymphocytes (MT-4). Cell viability was determined after 96 h at 37 °C by the 3-(4,5-dimethylthiazol-2-yl)-2,5-diphenyl-2*H*-tetrazolium bromide (MTT) method.[44]

Antiviral Activity (MTT Assay): Activity against YFV, DFV (type 2) and WNV was based on inhibition of virus-induced cytopathogenicity in acutely infected BHK-21 cells. Activity against BVDV was based on inhibition of virus-induced cytopathogenicity in acutely infected MDBK cells. After a 3-d incubation at 37 °C, the number of viable cells was determined by the MTT method.[44]

BVDV NS5B Expression and Purification: The expression plasmid encoding His-tagged C-terminal 24-amino-acid-deleted BVDV-NS5B was transformed into the *Escherichia coli* strain BL21 (DE3) Rosetta pLysS (Novagene). Transformants were treated as described in Experimental.

BVDV RNA-Dependent RNA Polymerase Assay: Compounds were dissolved in DMSO as 1 mM stocks and were then diluted in the buffer, as described in Experimental, and tested at the final concentration of 50 μM. The RdRp activity was measured on BVDV NS5B enzyme preparation, both in the absence or in the presence of test compounds.

Molecular Modeling All simulations were run on a cluster of Silicon Graphics Octane and performed by using the program packages AutoDock (v. 3.0)[45] AMBER 7.0,[46,47] Materials Studio (v. 3.2),[48] Discover[49] and in-house developed codes (stand-alone and add-on to the commercial software). The starting 3-D model of the RdRp was based on its X-ray crystallographic structure[50] (chain B, PBD Code: 1CSJ). The all-atom force field (FF) parameters by Cornell *et al.*[51] (in *parm94.dat* file of the AMBER 7.0 code) was applied in all simulations.

Each best drug/RdRp complex resulting from the application of validated docking procedures[52,53] was further refined in the AMBER suite using the quenched molecular dynamics method (QMD).[54] Extended molecular dynamics simulations at 25 °C were further conducted in the Molecular Mechanics/Poisson-Boltzmann Surface Area framework[55] to both qualify and quantify the interaction between the enzyme and the nucleoside analogs.

Results and Discussion

Notwithstanding the preliminary nature of these data, the study highlighted an interesting activity of several of the synthesized compounds (Tables 2, 3). Appreciable potency and selectivity have been achieved on BVDV by the introduction of hindering substituents at the sugar portion of ribo- and arabinofuranosyl nucleosides (**4**, **23**, **29**). However, among this latter only **29** might be considered an interesting lead compound. Indeed, **4** and **23** although active against BVDV displayed a cytotoxic concentration against MT-4 cells very close to antiviral concentration. Similar modifications on 2′-deoxyadenosine led to inactive or to highly cytotoxic derivatives (**7**, **8**).

Among the silyl groups the most effective in conferring inhibitory activity was the TBDPS in both ribo- and arabino-series. Anyway, whereas the TBDPS group at 5′-position of adenosine led to a quite active compound (**4**), effective arabinofuranosyl derivatives were obtained only by substitution of both 5′- and 2′-OH (**23**). On the contrary, bis-*O*-substitution at positions 3′- and 5′-OH (**22**) and tri-*O*-substitution at positions 2′-, 3′- and 5′-OH (**24**) were not effective.

Among the non-silyl groups, the triphenylmethyl was the most effective, but only in the arabinofuranosyl series (**28**, **29**). In particular, this substitution at 5′-position (**28**) induced moderate activity against BVDV, although associated to high cytotoxicity (Table 3).

The presence of an additional trityl group at N^6-position led to a consistent decrease of cytotoxicity and to mainte-

Table 2. Cytotoxicity and Antiviral Activities of Ribo- and Deoxyribo-adenosine Derivatives

Compounds	MT-4	YFV		BVDV		DFV-2, WNV	
	CC_{50} [a]	CC_{50} [a]	EC_{50} [b]	CC_{50} [a]	EC_{50} [b]	CC_{50} [a]	EC_{50} [b]
4	15	12	>12	>100	14	12	>12
5	14	17	>17	53	22	17	>17
6	10	8	5	16	11	8	>8
7	>100	37	>37	>100	>100	37	>37
8	>100	15	>15	20	>20	15	>15
9	>100	>100	>100	20	>20	ND	ND
10	41	6	>6	3.1	>3.1	ND	ND
11	14	4	>14	10	>10	ND	ND
12	>70	10	>10	3	>3	ND	ND
13	>100	>100	>100	>100	>100	ND	ND
14	>100	22	>22	10	>10	ND	ND
15	100	>100	>100	87	>87	ND	ND
16	>100	>100	>100	>100	>100	ND	ND
17	25	2.2	>2.2	53	>53	ND	ND

a) Compound concentration (μM) required to reduce the viability of mock-infected cells by 50%, as determined by the MTT or plaque reduction method. *b*) Compound concentration (μM) required to achieve 50% protection from virus-induced cytopathogenicity, as determined by the MTT method. ND: Not Detected

Table 3. Cytotoxicity and Antiviral Activities of araA Derivatives

Compounds	MT-4	YFV		BVDV		DFV-2, WNV	
	CC_{50} [a]	CC_{50} [a]	EC_{50} [b]	CC_{50} [a]	EC_{50} [b]	CC_{50} [a]	EC_{50} [b]
3	ND	90	>90	>100	>100	90	>90
18	87	>100	>100	>100	>100	>100	>100
19	26	58	>58	>100	>100	ND	ND
20	>100	>100	>100	>100	>100	>100	>100
21	>100	70	>70	>100	>100	70	>70
23	19	36	>36	>100	11	ND	ND
26	>100	60	>60	>100	>100	60	>60
27	>100	58	≥58	>72	>72	58	>58
28	25	82	22	72	21	62	>62
29	76	9	>9	>100	26	9	>9
30	>100	>100	>100	>100	>100	ND	ND
31	>100	>100	>100	>100	>100	ND	ND
32	>100	>100	>100	>100	>100	>100	>100
33	>100	>100	>100	>100	>100	>100	>100
34	>100	>100	>100	>100	>100	>100	>100
35	63	22	>22	22	>22	ND	ND
36	18	6	>6	9	>9	ND	ND

a) Compound concentration (μM) required to reduce the viability of mock-infected cells by 50%, as determined by the MTT or plaque reduction method. *b*) Compound concentration (μM) required to achieve 50% protection from virus-induced cytopathogenicity, as determined by the MTT method. ND: Not detected.

nance of the anti BVDV activity (**29**). Further modifications to a basic structure of compound **28** produced a complete loss of activity (**30**, **31**). Similar substitutions in ribofuranosyl series were not significant (**16**, **17**).

Inactive compounds were obtained when TBDMS, DPMS, tetrahydropyranyl (THP) and TIPDS groups were introduced in ribo-, deoxy- and arabinofuranosyl nucleosides (**9**—**15**, **18**—**20**, **25**—**27**, **32**—**36**).

A modest activity against YFV has been finally observed with compound **28** although associated with a high degree of cytotoxicity. The absence of effective treatment against this virus makes this data noteworthy and the compound structure suitable for further investigations.

As previously discussed all adenine compounds displaying a certain anti-BVDV activity present an arabino- or ribo-nucleoside structure, thus indicating the importance of the 2′-position. An important consideration also consists in the fact that whereas the activity of these compounds was discovered by serendipity, just testing synthetic intermediates, a specific role played by the silicon moiety should be taken into account. Indeed the silicon is an isoster of carbon and displays similar pharmacological properties but improved bioavailability.[56]

These results, that await further elucidations, also suggest that essential requisites for the activity are the specific sugar structure connected with the presence of the bulky groups on hydroxyl functions.

In order to further extend the structure–activity relationships, substitutions at position 8 of adenine and the replacement of adenine with other bases such as guanine and hypoxanthine are currently under investigation.

To assess our hypothesis with regard to the target, the selected compounds were finally evaluated for their activity on BVDV RdRp (Table 4). Enzyme assays demonstrated that the tested compounds inhibited the BVDV RNA-dependent RNA polymerase activity, thus confirming that the NS5B is their target. Particularly, our *in vitro* studies show that compounds **4**, **23**, **29** are active in inhibiting the BVDV RdRp activity

Table 4

Compound	ΔG_{bind} (kcal/mol) [a]	$IC_{50,calc}$ (μM) [a]	$IC_{50,found}$ (μM) [b]	ΔG_{bind} (kcal/mol) [c]	$IC_{50,calc}$ (μM) [c]
4	−6.50	17	27	−6.50	17
5	−6.58	15	30	−6.58	15
6	−6.82	9.9	32	−6.41	18
23	−6.76	11	16	−7.12	6
28	−5.98	41	37	−5.94	44
29	−6.62	14	15	−6.62	14
33	−5.05	199	>100	−4.97	227
34	−5.15	167	>100	−5.14	172

a) Free energy of binding ΔG_{bind} and IC_{50} values resulting from MM/PBSA calculations on BVDV NS5B in complex with a selected set of nucleoside analogs. *b*) BVDV RNA-dependent RNA polymerase inhibition activity (μM). *c*) Free energy of binding ΔG_{bind} and IC_{50} values resulting from MM/PBSA calculations on HCV NS5B in complex with a selected set of nucleoside analogs.

(IC_{50}=27, 16 and 15 mM respectively).

Moreover, Table 4 also reports the activity found on BVDV RdRp together with our estimates of the free energies of binding of the selected compounds to the allosteric surface site of the NS5B protein of BVDV, obtained by using the molecular mechanics poisson-boltzmann surface area (MM/PBSA) method. These data show that the applied computational strategy is able to yield absolute free energies of binding, and hence IC_{50} values, which are comparable to those obtained on the isolated enzyme.

Finally, free energy of binding and IC_{50} values resulting from MM/PBSA calculations on HCV NS5B in complex with the selected set of nucleoside analogs were also evaluated (Table 4). Preliminary molecular modeling studies revealed in fact a possible interaction of the inhibitors with a putative binding site at the HCV RdRp enzyme surface. Interestingly, we can also observe the good agreement between the trend exhibited by the IC_{50} values reported in Table 4 for HCV NS5B and the corresponding biological activity determined for these compounds in BVDV infected cell lines (Tables 2, 3). Data showed in Table 4 suggest that this class of

compounds is active against this important pathogen of the Flaviviridae family, and that its target can be reasonably identified in the RdRP.

These evidences, comforting *per se*, could be generally well justified considering that i) most of the amino acids making up the NS5B surface binding pocket are conservatively substituted between HCV and BVDV (*i.e.*, the interactions involved between a given residue and the drug can be easily replaced without a major penalty in the corresponding free energy of interaction), ii) some substitutions are located at a given position of the binding pocket (*e.g.*, the surface), where the drug/protein interactions may not be so critical, and iii) some of the most energetically favorable interactions (salt bridges and hydrogen bonds) between these nucleoside analogs and the RdRp involve backbone atoms of the enzymes. Accordingly, in this case it should not be a problem for an inhibitor to bind even in the presence of a non-conservative substitution.

To go further into the detailed knowledge of the interactions between the HCV NS5B RdRp and the inhibitors presented in this work, we will discuss a representative example, *i.e.* compound **23**. The nucleoside analog **23** occupies the central portion of the polymerase extended allosteric cleft, and the detailed interactions between **23** and the enzyme are illustrated in Fig. 2. The interface consists primarily of nonpolar surfaces, along with some hydrogen bonds. The most intimate interactions involve the phenyl and *tert*-butyl bulky substituents on the sugar ring, which fit into a hydrophobic region, lined by the side chains of M 423, W 528, L 419, Y 477 and R 422 (alkyl portion of the side chain). One edge of another phenyl ring of **23** rests on side chains of M 423 and L 419, while a further phenyl moiety is surrounded by the side chain of L 497 and W 500. The base is aptly lined by the polar residues S 476, S 478, P 479 and Y 477 (Fig. 2).

The component analysis of the free energy of binding of this compound towards the HCV NS5B is reported in Table 5.

As shown in Table 5, the intermolecular van der Waals and the electrostatics are both important contributions to the binding. However, the electrostatic desolvation penalty (ΔG_{PB}) offsets the favorable (negative) intermolecular electrostatics, yielding an unfavorable net electrostatic contribution to the binding. The calculated changes in solute entropy, $-T\Delta S_{solute}$, is physically reasonable. Indeed, the presence of the bulky, hydrophobic substituents at the sugar ring precludes large conformational freedom in this series of compounds, although the ligands are still endowed with some flexibility, so that they are able to place the different substituents and functional groups in slightly different locations relative to one another.

The above description of NS5B-inhibitor interactions applies, with minor modifications, to the other inhibitors. Further studies currently ongoing at our laboratories (*i.e.* inhibition of YFV polymerase, data not shown) also confirm this enzyme as the putative target of the observed activity in cells.

In conclusion, the present investigation shows that the degree of selectivity against the different viruses is connected with different substituents and the pattern of substitution (see **23** *versus* **28** and **29** and **5** *versus* **6**) thus envisaging the possibility to design selective agents. In our opinion these results open a new perspective in the development of anti-Flaviviridae agents possibly endowed with selectivity on the different members of this family of viruses. Of particular interest the fact that these results are predictive of a possible activity as anti-HCV agents that awaits further confirmation.

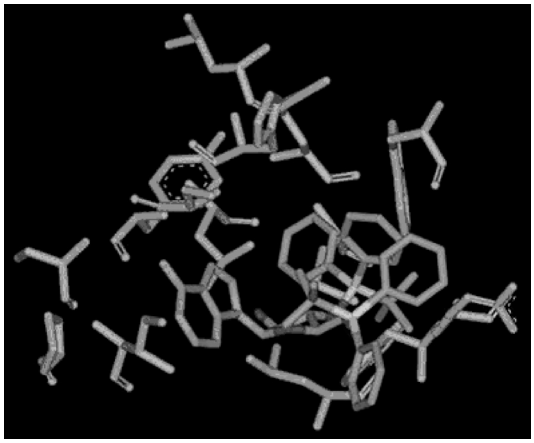

Fig. 2. Detailed Interactions between Compound **23** and the Residues Lining the Putative Binding Site of HCV NS5B

Table 5. Binding Free Energy Components for Compound **23**

Energy component	Values
ΔE_{EL}	−28.4
ΔE_{vdW}	−39.5
ΔE_{MM}	−67.9
ΔE_{NP}	−8.22
ΔE_{PB}	52.0
$\Delta E_{MM/PBSA}$	−24.1
$T\Delta S_{solute}$	17.0
ΔG_{bind}	−7.12

All values are in kcal/mol.

Experimental

Chemistry Reaction courses were routinely monitored by thin-layer chromatography (TLC) on silica gel precoated Macherey-Nagel durasil-25, with detection under a 254-nm UV lamp and/or by spraying the plates with 10% H_2SO_4/CH_3OH and heating. Column chromatography was performed with Macherey-Nagel 0.063—0.2 mm/70—230 mesh silica gel. MALDI-MS (Matrix-assisted laser desorption ionization time-of-flight) spectra were obtained on a Hewlett-Packard HPG2025A mass spectrometer operative in a positive linear mode. Nuclear magnetic resonance spectra were determined in DMSO-d_6, D_2O and $CDCl_3$ solution with a Varian VXR-200 MHz spectrometer or Varian MERCURY*plus* 400 MHz and chemical shifts are presented in ppm from internal tetramethylsilane as a standard. Melting points were determined by Kofler melting point apparatus (Thermovar, C. Reichert AG, Vienna) and are uncorrected. Microanalyses, unless indicated, were in agreement with calculated values within ±0.4%. All drying operations were performed over anhydrous sodium sulphate or magnesium sulphate; room temperature varied between 22 and 25 °C.

General Synthetic Procedure for the Preparation of 5′-*O*-Silyl Derivatives (4, 8, 15, 18, 21, 25) 5′-*O*-Silyl-derivatives were easily prepared starting from dry adenosine, deoxyadenosine or araA (1 mmol), suspended in dry pyridine (2 ml), by treatment with the selected silylating agent (1.25 mmol), as previously described by Ogilvie *et al*. for the adenosine silylation.[27]

5′-*O*-(*tert*-Butyldiphenylsilyl)adenosine (4) The crude product was purified by silica gel column chromatography (eluent: CH_2Cl_2/MeOH, 100/0→90/10, v/v), to give **4** (404 mg, 80%) as a white solid (mp 197—198 °C).[29]

5′-*O*-(*tert*-Butyldiphenylsilyl)-2′-deoxyadenosine (8) The crude product was purified by silica gel column chromatography (eluent: CH_2Cl_2/

MeOH, 100/0→95/05, v/v), to give **8** (367 mg, 75%) as a white foam. ^{1}H-NMR (DMSO-d_6) δ (ppm): 0.96 (s, 9H, *t*But–Si); 2.30—2.39 (m, 1H, H2′); 2.77—2.86 (m, 1H, H2″); 3.73 (part of ABX system, 1H, $J_{A\text{-}B}$=10.2 Hz, $J_{A\text{-}X}$=4.6 Hz, H5′); 3.87—4.00 (m, 2H, H5″, H4′); 4.50—4.60 (m, 1H, H3′); 5.42 (d, 1H, J=4.2 Hz, OH3′); 6.37 (t, 1H, J=13.0 Hz, H1′); 7.30—7.61 (m, 12H, 4×Ph–Si and NH_2); 8.08 (s, 1H, H2); 8.25 (s, 1H, H8). MALDI-TOF MS *m*/*z*: 490.8 Da [M+H]; 512.7 Da [M+Na]$^+$; 528 Da [M+K]$^+$; *Anal.* Calcd for $C_{26}H_{31}N_5O_3Si$: C, 63.78; H, 6.38; N, 14.30. Found: C, 63.50; H, 6.38; N, 14.30.

5′-*O*-(*tert*-Butyldimethylsilyl)adenosine (15) The crude product was purified by silica gel column chromatography (eluent: CH_2Cl_2/MeOH, 100/0→95/05, v/v), to give **15** (316 mg, 83%) as a white solid (mp 178—180 °C).[30]

9-[5′-*O*-(*tert*-Butyldimethylsilyl)-β-D-arabinofuranosyl]adenine (18) The crude product was purified by silica gel column chromatography (eluent: CH_2Cl_2/MeOH, 100/0→90/10, v/v), to give **18** (282 mg, 74%) as a white solid (mp 157—158 °C). ^{1}H-NMR (DMSO-d_6) δ (ppm): 0.83 (s, 6H, 2×Me–Si); 1.00 (s, 9H, *t*But–Si); 3.72—3.81 (m, 3H, H5′, H5″, H4′); 4.06—4.16 (m, 2H, H3′, H2′); 5.51 (d, 1H, J=4.5 Hz, OH3′); 5.61 (d, 1H, J=5.0 Hz, OH2′); 6.19 (d, 1H, J=5.0 Hz, H1′); 7.21 (br s, 2H, NH_2); 8.07 (s, 1H, H2); 8.07 (s, 1H, H8). MALDI-TOF MS *m*/*z*: 382.4 Da [M+H]; 404.2 Da [M+Na]$^+$; *Anal.* Calcd for $C_{16}H_{27}N_5O_4Si$: C, 50.37; H, 7.13; N, 18.36. Found: C, 50.38; H, 7.10; N, 18.35.

9-[5′-*O*-(*tert*-Butyldiphenylsilyl)-β-D-arabinofuranosyl]adenine (21) The crude product was purified by silica gel column chromatography (eluent: CH_2Cl_2/MeOH, 100/0→90/10, v/v), to give **21** (383 mg, 76%) as a white solid (mp 89—93 °C).[29]

9-[5′-*O*-(Methyldiphenylsilyl)-β-D-arabinofuranosyl]adenine (25) The crude product was purified by silica gel column chromatography (eluent: CH_2Cl_2/MeOH, 100/0→90/10, v/v), to give **25** (372 mg, 78%) as a white solid (mp 168—172 °C). ^{1}H-NMR (DMSO-d_6) δ (ppm): 0.62 (s, 3H, Me–Si); 3.86—3.90 (m, 3H, H5′, H5″, H4′); 4.17—4.20 (m, 2H, H3′, H2′); 5.61 (d, 1H, J=3.8 Hz, OH3′); 5.69 (d, 1H, J=4.5 Hz, OH2′); 6.27 (d, 1H, J=4.1 Hz, H1′); 7.24—7.56 (m, 12H, 2×Ph–Si and NH_2); 8.06 (s, 1H, H2); 8.13 (s, 1H, H8). MALDI-TOF MS *m*/*z*: 464.8 Da [M+H]; 486.7 Da [M+Na]$^+$; 502.1 Da [M+K]$^+$; *Anal.* Calcd for $C_{23}H_{25}N_5O_4Si$: C, 59.59; H, 5.44; N, 15.11. Found: C, 59.58; H, 5.43; N, 15.11.

General Synthetic Procedure for the Preparation of TIPDS Derivatives (11, 12, 35, 36) 3′,5′-*O*-TIPDS derivatives of adenosine, 2′-deoxyadenosine or araA were obtained by treatment of the dry nucleoside (1 mmol), suspended in pyridine (10 ml), with 1,3-dichloro-1,1,3,3-tetraisopropyldisiloxane ($TIPDSCl_2$) (1 mmol), following a synthetic procedure previously described.[34] Starting from araA, by a one-step reaction, both **35** and **36** were obtained. The crude products were purified by silica gel column chromatography (eluent: CH_2Cl_2/MeOH, 100/0→97/03, v/v).

3′,5′-*O*-(1,1,3,3-Tetraisopropyldisiloxane-1,3-diyl)adenosine (11) Yield 80%; white foam.[35]

3′,5′-*O*-(1,1,3,3-Tetraisopropyldisiloxane-1,3-diyl)-2′-deoxyadenosine (12) Yield 81%; white foam.[36]

9-[5′-*O*-(1-Hydroxy-1,1,3,3-tetraisopropyl-disiloxanyl)-β-D-arabinofuranosyl]adenine (35) Yield 15%; white solid (mp 160—165 °C). ^{1}H-NMR (DMSO-d_6) δ (ppm): 0.76—1.11 (m, 28H, TIPDS); 3.80—3.83 (m, 1H, H5′); 3.95—3.96 (m, 2H, H5″, H4′); 4.15—4.25 (m, 2H, H3′, H2′); 5.55 (d, 1H, J=4.3 Hz, OH3′); 5.65 (d, 1H, J=3.9 Hz, OH2′); 6.08 (s, 1H, Si–OH); 6.25 (d, 1H, J=4.1 Hz, H1′); 7.25 (br s, 2H, NH_2); 8.08 (s, 1H, H2); 8.12 (s, 1H, H8). MALDI-TOF MS *m*/*z*: 529.1 Da [M+H]; 551.1 Da [M+Na]$^+$; 566.3 Da [M+K]$^+$; *Anal.* Calcd for $C_{22}H_{41}N_5O_6Si_2$: C, 50.07; H, 7.83; N, 13.27. Found: C, 49.93; H, 7.81; N, 13.30.

9-[3′,5′-*O*-(1,1,3,3-Tetraisopropyldisiloxane-1,3-diyl)-β-D-arabinofuranosyl]adenine (36) Yield 57%; white foam.[37]

3′,5′-Bis-*O*-(*tert*-butyldiphenylsilyl)adenosine and 2′,5′-Bis-*O*-(*tert*-butyldiphenylsilyl) adenosine (5, 6) Bis-silylated compounds **5** and **6** were obtained by treatment of dry adenosine (1 mmol), dissolved in dry DMF (1 ml), with imidazole (4.4 mmol) and *tert*-butyldiphenylsilyl chloride (TBDPSCl) (2.2 mmol). The crude mixture was purified by silica gel column chromatography (eluent: CH_2Cl_2/MeOH, 100/0→95/5, v/v) to give 297 mg and 222 mg of compounds **5** and **6** respectively.

5: Yield 40%; white foam. ^{1}H-NMR (DMSO-d_6) δ (ppm): 0.83 and 1.09 (s, 18H, 2×*t*But–Si); 3.21—3.29 (m, 1H, H5′); 3.50—3.63 (m, 1H, H5″); 3.99—4.02 (m, 1H, H4′); 4.48—4.51 (m, 1H, H3′); 4.75—4.78 (m, 1H, H2′); 5.72 (d, 1H, J=6.6 Hz, OH2′); 6.05 (d, 1H, J=6.6 Hz, H1′); 7.29—7.73 (m, 24H, 4×Ph–Si, NH_2, H2, H8). MALDI-TOF MS *m*/*z*: 745.6 Da [M+H]; 767.4 Da [M+Na]$^+$; 783.0 Da [M+K]$^+$; *Anal.* Calcd for $C_{42}H_{49}N_5O_4Si_2$: C, 67.82; H, 6.64; N, 9.41. Found: C, 67.82; H, 6.62; N, 9.43.

6: Yield 30%; white foam. ^{1}H-NMR (DMSO-d_6) δ (ppm): 0.86 and 0.93 (s, 18H, 2×*t*But–Si); 3.72—3.64 (m, 1H, H5′); 3.82—3.85 (m, 1H, H5″); 4.13—4.25 (m, 2H, H4′, H3′); 4.80—4.90 (m, 1H, H2′); 5.46 (d, 1H, J=6.1 Hz, OH3′); 6.10 (d, 1H, J=6.0 Hz, H1′); 7.05—7.62 (m, 22H, 4×Ph–Si and NH_2); 7.93 (s, 1H, H2); 7.96 (s, 1H, H8). MALDI-TOF MS *m*/*z*: 745.6 Da [M+H]; 767.4 Da [M+Na]$^+$; 783.0 Da [M+K]$^+$; *Anal.* Calcd for $C_{42}H_{49}N_5O_4Si_2$: C, 67.80; H, 6.64; N, 9.41. Found: C, 67.90; H, 6.63; N, 9.42.

3′,5′-Bis-*O*-(*tert*-butyldiphenylsilyl)-2′-deoxyadenosine (7) Compound **7** was obtained as described for compounds **5** and **6** starting from deoxyadenosine. The crude product was purified by silica gel column chromatography (eluent: CH_2Cl_2/MeOH, 100/0→97/3, v/v) to afford compound **7** (426 mg, 59%) as a white foam. ^{1}H-NMR (DMSO-d_6) δ (ppm): 0.82 and 1.05 (s, 18H, 2×*t*But–Si); 2.35—2.40 (m, 1H, H2′); 2.73—2.81 (m, 1H, H2′); 3.40—3.50 (m, 1H, H5′); 3.66 (part of ABX system, 1H, $J_{A\text{-}B}$= 11.2 Hz, $J_{B\text{-}X}$=4.8 Hz, H5″); 4.09—4.12 (m, 1H, H4′); 4.68—4.72 (m, 1H, H3′); 6.43 (t, 1H, J=6.5 Hz, H1′); 7.29—7.64 (m, 22H, 4×Ph–Si and NH_2); 8.00 (s, 1H, H2); 8.13 (s, 1H, H8). MALDI-TOF MS *m*/*z*: 729.5 Da [M+H]; 789.5 Da [M+Na+K]$^+$; *Anal.* Calcd for $C_{42}H_{49}N_5O_3Si_2$: C, 69.29; H, 6.78; N, 9.62. Found: C, 69.27; H, 6.75; N, 9.61.

Preparation of N^6-*tert*-Butyldimethylsilyl-3′,5′-bis-*O*-(*tert*-butyldimethylsilyl)-2′-deoxyadenosine and 3′,5′-Bis-*O*-(*tert*-butyldimethylsilyl)-2′-deoxyadenosine (9, 10) Compounds **9** and **10** were prepared following the synthetic strategy described for compounds **5** and **6** starting form deoxyadenosine and TBDMSCl. The crude mixture was purified by silica gel column chromatography (eluent: Hexane/EtOAc, 95/05→70/30, v/v), to give compounds **9** and **10**.

9: Yield 4%; white oil. ^{1}H-NMR (DMSO-d_6) δ (ppm): −0.06, −0.01, 0.00, 0.01, 0.11 and 0.31 (s, 18H, 6×Me–Si); 0.83, 0.84 and 0.96 (s, 27H, 3×*t*But–Si); 2.26—2.32 (m, 1H, H2′); 2.86—3.00 (m, 1H, H2″); 3.60—3.70 (m, 1H, H5′); 3.76—3.84 (m, 2H, H5″, H4′); 4.60—4.68 (m, 1H, H3′); 6.30—6.37 (m, 2H, H1′, 6-NH); 8.21 (s, 1H, H2); 8.32 (s, 1H, H8). MALDI-TOF MS *m*/*z*: 595.5 Da [M+H]; 617.4 Da [M+Na]$^+$; 633.5 Da [M+K]$^+$; *Anal.* Calcd for $C_{28}H_{55}N_5O_3Si_3$: C, 56.61; H, 9.33; N, 11.79. Found: C, 56.68; H, 9.33; N, 11.75.

10: Yield 70%; white solid (mp 125—128 °C).[31]

3′,5′-Bis-*O*-(*tert*-butyldimethylsilyl)adenosine and 2′,5′-Bis-*O*-(*tert*-butyldimethylsilyl)adenosine (13, 14) Compounds **13** and **14** were obtained as described for compounds **5** and **6**. The crude mixture purified by silica gel column chromatography (eluent: CH_2Cl_2/MeOH, 100/0→95/05, v/v), gave pure compounds **13**, **14**.

13: Yield 36%; white solid (mp 202—204 °C).[32]

14: Yield 19%; white solid (mp 174—177 °C).[32]

Preparation of 9-(3′,5′-Bis-*O*-TBDPS), 9-(2′,5′-Bis-*O*-TBDPS) and 9-(2′,3′,5′-Tri-*O*-TBDPS-β-D-arabinofuranosyl)adenine (22, 23, 24) Compounds **22**—**24** were prepared by a one step reaction starting form araA and TBDPSCl following the synthetic strategy previously reported for the preparation of compounds **5** and **6**. The crude mixture was purified by silica gel column chromatography (eluent: CH_2Cl_2/MeOH, 98/2→97/3, v/v), to give pure compounds **22**—**24**.

22: Yield 12%; white solid (mp 219—225 °C). ^{1}H-NMR (400 MHz, DMSO-d_6) δ (ppm): 0.84 and 1.06 (s, 18H, 2×*t*But–Si); 3.47, 3.59 (part of AB system, 2H, $J_{A\text{-}B}$=10.8 Hz, $J_{A\text{-}X}$=4.4 Hz, $J_{B\text{-}X}$=6.8 Hz, H5′, H5″); 4.07—4.11 (m, 1H, H4′); 4.26—4.28 (m, 1H, H2′); 4.36—4.38 (m, 1H, H3′); 5.78 (d, 1H, J =4.8 Hz, OH2′); 6.41 (d, 1H, J=4.0 Hz, H1′); 7.27—7.64 (m, 22H, 4×Ph–Si and NH_2); 7.91 (s, 1H, H2); 8.13 (s, 1H, H8). MALDI-TOF MS *m*/*z*: 745.2 Da [M+H]; 767.4 Da [M+Na]$^+$; 783.3 Da [M+K]$^+$; *Anal.* Calcd for $C_{42}H_{49}N_5O_4Si_2$: C, 67.80; H, 6.64; N, 9.41. Found: C, 67.91; H, 6.62; N, 9.42.

23: Yield 10%; white foam. ^{1}H-NMR (400 MHz, DMSO-d_6) δ (ppm): 0.80 and 1.03 (s, 18H, 2×*t*But–Si); 3.93—4.01 (m, 3H, H5′, H5″, H4′) 4.30—4.32 (m, 1H, H3′); 4.39—4.43 (m, 1H, H2′); 5.29 (d, 1H, J=5.2 Hz, OH3′); 6.24 (d, 1H, J=4.8 Hz, H1′); 6.90 (s, 2H, NH_2); 7.12—7.66 (m, 20H, 4×Ph–Si); 7.99 (s, 1H, H2); 8.08 (s, 1H, H8). MALDI-TOF MS *m*/*z*: 745.3 Da [M+H]; 767.1 Da [M+Na]$^+$; 783.1 Da [M+K]$^+$; *Anal.* Calcd for $C_{42}H_{49}N_5O_4Si_2$: C, 67.80; H, 6.64; N, 9.41. Found: C, 67.78; H, 6.63; N, 9.44.

24: Yield 10%; white foam. ^{1}H-NMR (400 MHz, DMSO-d_6) δ (ppm): 0.54, 0.92 and 0.94 (s, 27H, 3×*t*But–Si); 3.04 (A part of ABX system, 1H, $J_{A\text{-}B}$=10.8 Hz, $J_{A\text{-}X}$=4.0 Hz, H5′); 3.67—3.72 (m, 1H, H5″); 3.88 (s, 1H, H3′); 4.26 (part of ABX system, 1H, $J_{X\text{-}B}$=8.4 Hz, $J_{X\text{-}A}$=4.0 Hz, H4′); 4.31 (d, 1H, $J_{2'\text{-}1'}$=2.8 Hz, H2′); 6.49 (d, 1H, $J_{1'\text{-}2'}$=2.8 Hz, H1′); 6.82 (d, 2H, J=7.2 Hz, NH_2); 6.96—8.00 (m, 30H, 6×Ph–Si); 7.96 (s, 1H, H2); 8.17 (s,

1H, H8). MALDI-TOF MS *m/z*: 983.3 Da [M+H]; 1006.1 Da [M+Na]$^+$; *Anal.* Calcd for $C_{58}H_{67}N_5O_4Si_3$: C, 70.91; H, 6.87; N, 7.13. Found: C, 71.23; H, 6.86; N, 7.17.

9-[2′,5′-Bis-*O*-(methyldiphenyl)-β-D-arabinofuranosyl]adenine and 9-[2′,3′,5′-Tri-*O*-(methyldiphenyl)-β-D-arabinofuranosyl]adenine (26, 27) Compounds **26** and **27** were obtained as described for compounds **5** and **6** by simple substitution of the silylating agent. The crude products were purified by silica gel column chromatography (eluent: CH_2Cl_2/MeOH, 100/0→80/20, v/v) to give **26** and **27**.

26: Yield 41%; white foam. ^{1}H-NMR (DMSO-d_6) δ (ppm): 0.42 and 0.61 (s, 6H, 2×Me–Si); 3.92—3.98 (m, 3H, H5′, H5″, H4′); 4.32—4.40 (m, 2H, H3′, H2′); 5.73 (d, 1H, *J*=4.7 Hz, OH3′); 6.30 (d, 1H, *J*=4.5 Hz, H1′); 7.05—7.56 (m, 22H, 4×Ph–Si and NH_2); 8.08 (br s, 2H, H2, H8). MALDI-TOF MS *m/z*: 660.9 Da [M+H]; 682.8 Da [M+Na]$^+$; *Anal.* Calcd for $C_{36}H_{37}N_5O_4Si_2$: C, 65.52; H, 5.65; N, 10.16. Found: C, 65.31; H, 5.62; N, 10.14.

27: Yield 18%; white foam. ^{1}H-NMR (DMSO-d_6) δ (ppm): 0.11, 0.48 and 0.52 (s, 9H, 3×Me–Si); 3.75—3.78 (m, 2H, H5′, H5″); 4.09—4.10 (m, 1H, H4′); 4.38—4.41 (m, 1H, H2′); 4.58—4.59 (m, 1H, H3′); 6.35 (d, 1H, *J*=4.0 Hz, H1′); 7.16—7.50 (m, 32H, 6×Ph–Si and NH_2); 7.93 (s, 1H, H2); 8.06 (s, 1H, H8). MALDI-TOF MS *m/z*: 857.3 Da [M+H]; 879.0 Da [M+Na]$^+$; 895.2 Da [M+K]$^+$; *Anal.* Calcd for $C_{49}H_{49}N_5O_4Si_3$: C, 68.74; H, 5.77; N, 8.18. Found: C, 68.71; H, 5.77; N, 8.23.

9-[2′,3′,5′-Tri-*O*-(*tert*-butyldimethylsilyl)-β-D-arabinofuranosyl)adenine (20) Compound **20** was prepared as described in literature.[34]

9-[2′,5′-Bis-*O*-(*tert*-butyldimethylsilyl)-β-D-arabinofuranosyl]adenine (19) Compound **19** was obtained by the reaction of dry araA (1 mmol) dissolved in THF (20 ml) with TBDMSCl (2.2 mmol) in presence of DABCO (6 mmol) and $AgNO_3$ (1 mmol) as described in 1982 by Ogilvie *et al.*[28] Yield 60%; white solid (mp 190—191 °C).[33]

***N*^{6}-Triphenylmethyl-(5′-*O*-triphenylmethyl)adenosine and 5′-*O*-Triphenylmethyladenosine (16, 17)** Compound **16** was prepared, as described in literature,[39] treating adenosine (5 mmol) with triphenylmethyl chloride (15 mmol) in pyridine (15 ml) at 50 °C overnight. The crude mixture was purified by silica gel column chromatography (eluent: CH_2Cl_2/MeOH, 100/0→95/05, v/v) to give pure compound **16** and a fair amount of compound **17**.

16: Yield 51%; white solid (mp 216—218 °C).[39]

17: Yield 38%; white solid (mp 119—122 °C)[40]

9-(5′-*O*-Triphenylmethyl-β-D-arabinofuranosyl)adenine (28) Compound **28** was prepared treating araA (0.374 mmol) dissolved in pyridine (20 ml), with trityl chloride (0.78 mmol) for 3 d at 50 °C, following and adapting a literature reported synthetic procedure.[42] The crude compound was purified by silica gel column chromatography (eluent: CH_2Cl_2/MeOH, 100/0→95/05v/v) to give **28** (0.135 mg, 36%) as a white foam. ^{1}H-NMR (DMSO-d_6) δ (ppm): 3.12—3.16 (m, 1H, H5′); 3.38—3.46 (m, 1H, H5″); 3.97—4.02 (m, 1H, H4′); 4.11—4.18 (m, 2H, H3′, H2′); 5.58 (d, 1H, *J*=3.8 Hz, OH3′); 5.68 (d, 1H, *J*=4.1 Hz, OH2′); 6.29 (d, 1H, *J*=3.9 Hz, H1′); 7.19—7.47 (m, 31H, 2×Ph_3C and 6-NH); 7.87 (s, 1H, H2); 8.12 (s, 1H, H8). MALDI-TOF MS *m/z*: 752.3 Da [M+H]; 774.6 Da [M+Na]$^+$; 790.9 Da [M+K]$^+$; *Anal.* Calcd for $C_{29}H_{27}N_5O_4$: C, 68.36; H, 5.34; N, 13.74. Found: C, 68.58; H, 5.34; N, 13.71.

***N*^{6}-Triphenylmethyl-9-(5′-*O*-triphenylmethyl-β-D-arabinofuranosyl)-adenine (29)** A solution of araA (200 mg, 0.75 mmol) and triphenylmethyl chloride (243 mg, 0.87 mmol) in dry pyridine (15 ml) was stirred for 1 h at 50 °C under argon atmosphere. Triphenylmethyl bromide (287 mg, 0.89 mmol) was then added and the mixture stirred for a further 2 h 30′ at 70 °C. After evaporation of the solvent the residue dissolved in CH_2Cl_2 was washed with cold aqueous 1 N HCl (20 ml), H_2O (20 ml), aqueous saturated $NaHCO_3$ (20 ml), brine (20 ml), and finally dried and evaporated to dryness. The residue purified by silica gel column chromatography (eluent: CH_2Cl_2/MeOH, 100/0→95/05 with 5 drops/l of TEA, v/v), gave compound **29** (110 mg, 20%), as a white solid (mp 140—145 °C). ^{1}H-NMR (DMSO-d_6): δ (ppm) 3.12—3.16 (m, 1H, H5′); 3.38—3.46 (m, 1H, H5″); 3.97—4.02 (m, 1H, H4′); 4.11—4.18 (m, 2H, H3′, H2′); 5.58 (d, 1H, *J*=3.8 Hz, OH3′); 5.68 (d, 1H, *J*=4.1 Hz, OH2′); 6.29 (d, 1H, *J*=3.9 Hz, H1′); 7.19—7.47 (m, 31H, 2×Ph_3C and NH); 7.87 (s, 1H, H2); 8.12 (s, 1H, H8). MALDI-TOF MS: *m/z* 752.3 Da [M+H]; 774.6 Da [M+Na]$^+$; 790.9 Da [M+K]$^+$; *Anal.* Calcd for $C_{48}H_{41}N_5O_4$: C, 76.68; H, 5.50; N, 9.31. Found: C, 76.75; H, 5.50; N, 9.31.

Preparation of *N*^{6}-Triphenylmethyl-9-[5′-*O*-triphenylmethyl-3′-*O*-(*tert*-butyldimethylsilyl)-β-D-arabinofuranosyl]adenine (31) To a solution of compound **29** (78 mg, 0.1 mmol) in anhydrous DMF (2 ml), TBDMSCl (30 mg, 0.2 mmol) and imidazole (27 mg, 0.4 mmol) were added. The mixture was stirred for 12 h at room temperature under argon atmosphere, then the solvent was evaporated, and co-evaporated with toluene. The obtained residue dissolved in EtOAc (20 ml) was washed with H_2O (2×20 ml) and the organic layer dried, filtered and evaporated. The crude product was purified by silica gel column chromatography (eluent: CH_2Cl_2/MeOH, 100/0→99/01 with 5 drops/l of TEA, v/v), to give compound **31** (28 mg, 32%) as a white solid (mp 122—125 °C). ^{1}H-NMR (400 MHz, DMSO-d_6) δ (ppm): −0.05 and 0.04 (s, 6H, 2×Me–Si); 0.78 (s, 9H, *t*But–Si); 3.25—3.40 (m, 2H, H5′, H5″); 3.89—3.94 (m, 1H, H4′); 4.16—4.21 (m, 1H, H2′); 4.35—4.38 (m, 1H, H3′); 5.73—5.77 (m, 1H, OH2′); 6.29 (s, 1H, *J*=5.4 Hz, H1′); 7.20—7.39 (m, 45H, 2×Ph_3C); 7.46 (s, 1H, NH); 7.89 (s, 1H, H2); 8.19 (s, 1H, H8). MALDI-TOF MS *m/z*: 899.6 Da [M+H]; *Anal.* Calcd for $C_{52}H_{55}N_5O_4Si$: C, 74.88; H, 6.40; N, 8.09. Found: C, 74.75; H, 6.37; N, 8.06.

***N*^{6}-Triphenylmethyl-9-(3′,5′-Bis-*O*-triphenylmethyl-β-D-arabinofuranosyl)adenine (30)** A mixture of araA (100 mg, 0.37 mmol) and triphenylmethyl bromide (505 mg, 1.56 mmol) in dry pyridine (7.5 ml) was stirred for 4 h at 105 °C under argon atmosphere. Then, to the stirred mixture, a further addition of triphenylmethyl bromide (163 mg, 0.50 mmol) was made. After 1 h the solvent was evaporated and the residue dissolved in CH_2Cl_2 (20 ml), was washed with cold aqueous 1 N HCl (20 ml), H_2O (20 ml), aqueous saturated $NaHCO_3$ (20 ml), and brine (20 ml), and finally dried and evaporated. The residue was purified by silica gel column chromatography (eluent: CH_2Cl_2/MeOH, 100/0→97/03 with 5 drops/l of TEA, v/v), to give compound **30** (150 mg, 41%), as a pale yellow foam. ^{1}H-NMR (DMSO-d_6) δ (ppm): 3.17—3.20 (m, 1H, H5′); 3.39—3.46 (m, 1H, H5″); 3.62—3.70 (m, 1H, H3′); 3.89—3.94 (m, 1H, H4′); 4.21—4.26 (m, 1H, H2′); 5.06 (s, 1H, OH2′); 5.85 (s, 1H, *J*=4.6 Hz, H1′); 6.97—7.40 (m, 46H, 3×Ph_3C and NH); 7.82 (s, 1H, H2); 8.09 (s, 1H, H8). MALDI-TOF MS *m/z*: 995.6 Da [M+H]; 1033.5 Da [M+K]$^+$; *Anal.* Calcd for $C_{67}H_{55}N_5O_4$: C, 80.94; H, 5.58; N, 7.04. Found: C, 80.99; H, 5.56; N, 7.02.

9-(5′-*O*-Tetrahydropyranyl-β-D-arabinofuranosyl)adenine and 9-(3′,5′-Bis-*O*-tetrahydropyranyl-β-D-arabinofuranosyl)adenine (32, 33) A solution of araA (150 mg, 0.56 mmol) and *p*-toluensulfonic acid monohydrate (105 mg, 0.56 mmol) in anhydrous DMF (20 ml) was cooled to 5 °C and 3,4-dihydro-2*H*-pyran (DHP) (101 μl, 1.13 mmol) was added under an argon atmosphere. The reaction mixture was then allowed to warm to room temperature. Over a period of 5 h, a total of 10 eq of DHP were added, in 2 equal portions in the fashion described. After 19 h the reaction mixture cooled to 5 °C, was treated with saturated $NaHCO_3$/H_2O up to pH 8, and then with 30 ml H_2O. The aqueous mixture was extracted with CH_2Cl_2 (4×20 ml) and the organic layers combined, dried, filtered and evaporated. The residue was purified by silica gel column chromatography (eluent: CH_2Cl_2/MeOH, 98/02→90/10, v/v) to give compound **32** and compound **33**.

32: Yield 74%; white solid (mp 95—97 °C). ^{1}H-NMR (DMSO-d_6) δ (ppm): 1.46—1.70 (m, 6H, 3×CH_2 THP); 3.34—3.93 (m, 7H, CH_2O THP, CHO THP, H5′, H5″, H4′, H3′); 4.63—4.65 (m, 1H, H2′); 5.60—5.69 (m, 2H, OH3′, OH2′); 6.26 (d, 1H, *J*=4.8 Hz, H1′); 7.26 (br s, 2H, NH_2); 8.13 (s, 1H, H2); 8.16 (s, 1H, H8). MALDI-TOF MS *m/z*: 352.5 Da [M+H]; 374.3 Da [M+Na]$^+$; 390.3 Da [M+K]$^+$; *Anal.* Calcd for $C_{15}H_{21}N_5O_5$: C, 51.28; H, 6.02; N, 19.93. Found: C, 51.02; H, 6.01; N, 19.91.

33: Yield 11%; white solid (mp 66—68 °C). ^{1}H-NMR (DMSO-d_6) δ (ppm): 1.40—1.60 (m, 12H, 6×CH_2 THP); 3.64—4.90 (m, 11H, 2×CH_2O THP, 2×CHO THP, H5′, H5″, H4′, H3′, H2′); 5.80—5.84 (m, 1H, OH2′); 6.22—6.27 (m, 1H, H1′); 7.28 (br s, 2H, NH_2); 8.13—8.27 (s, 2H, H2, H8). MALDI-TOF MS *m/z*: 436.5 Da [M+H]; 458.8 Da [M+Na]$^+$; 474.2 Da [M+K]$^+$; *Anal.* Calcd for $C_{20}H_{29}N_5O_6$: C, 55.16; H, 6.71; N, 16.08. Found: C, 55.18; H, 6.71; N, 16.13.

9-[2′,3′,5′-Tri-*O*-(tetrahydropyranyl)-β-D-arabinofuranosyl]adenine (34) To a solution of AraA (150 mg, 0.56 mmol) and *p*-toluensulfonic acid monohydrate (105 mg, 0.56 mmol) in anhydrous DMF (20 ml), was added DHP (1 ml, 11.20 mmol) under an argon atmosphere. The mixture, stirred overnight at room temperature, was cooled to 5 °C, treated with aqueous saturated $NaHCO_3$ up to pH 8 and then with H_2O (30 ml). The aqueous layer was extracted with CH_2Cl_2 (4×30 ml), dried over anhydrous Na_2SO_4, filtered and finally evaporated to dryness. The residue was purified by silica gel column chromatography (eluent: CH_2Cl_2/MeOH, 98/02→90/10, v/v), to afford compound **34** (116 mg, 40%) as a white solid (mp 68—70 °C). ^{1}H-NMR (DMSO-d_6, 80 °C) δ (ppm): 1.23—1.75 (m, 18H, 9×CH_2 THP); 3.45—4.80 (m, 14H, 3×CH_2O THP, 3×CHO, H5′, H5″, H4′, H3″, H2′); 6.35—6.40 (m, 1H, H1′); 7.30—7.33 (m, 2H, NH_2); 8.14 (s, 1H, H2); 8.16 (s, 1H, H8). MALDI-TOF MS *m/z*: 520.8 Da [M+H]; 542.6 Da [M+Na]$^+$; 558.8 Da [M+K]$^+$; *Anal.* Calcd for $C_{25}H_{37}N_5O_7$: C, 57.79; H, 7.18; N, 13.48. Found: C, 57.65; H, 7.17; N, 13.49.

Biology Test compounds were dissolved in DMSO at 100 mM and then diluted in culture medium.

Cytotoxicity: Exponentially growing human $CD4^+$ lymphocytes (MT-4), baby hamster kidney (BHK-21), and Madin Darby bovine kidney (MDBK) cells were resuspended in growth medium containing serial dilutions of the drugs. Cell viability was determined after 96 h at 37 °C by the 3-(4,5-dimethylthiazol-2-yl)-2,5-diphenyl-tetrazolium bromide (MTT) method.[44]

Antiviral Activity (MTT Assay): Activity against YFV, DFV (type 2) and WNV was based on inhibition of virus-induced cytopathogenicity in acutely infected BHK-21 cells. Activity against BVDV was based on inhibition of virus-induced cytopathogenicity in acutely infected MDBK cells. Cells were seeded overnight at a rate of 5×10^4/well into 96-well plates in growth medium at 37 °C, in a humidified CO_2 (5%) atmosphere. Cell monolayers were infected with 50 μl of a proper virus dilution to give an MOI of 0.01. Then, serial dilutions of test compounds in Dulbecco's modified Eagle's medium, supplemented with 2% inactivated fetal calf serum, were added. After a 3-d incubation at 37 °C, the number of viable cells was determined by the MTT method.[39]

Expression and Purification of BVDV NS5B: The expression plasmid encoding the His-tagged C-terminal 24-amino-acid-deleted BVDV-NS5B was transformed into the *Escherichia coli* strain BL21 (DE3) Rosetta pLysS (Novagene), and the transformants were then cultured in 5 ml of LB medium with 25 μg/ml kanamycin and 30 μg/ml chloramphenicol at 30 °C overnight. Cultures were diluted into 0.25 l of LB medium with 25 μg/ml Kanamycin and 30 μg/ml chloramphenicol and incubated at 30 °C until the A600 reached 0.6—0.7. These cultures were then induced overnight with 2 mM isopropyl-β-D-thiogalactopyranoside. The cells (from 0.25 l) were harvested by centrifugation, and cell lysis was achieved by the addition of 10 ml of CelLytic B (Sigma). Any insoluble material was removed by centrifugation at 11000 rpm (4 °C) for 60 min. The soluble extract was applied to a 5-ml column of nickel-nitrilotriacetic acid-agarose (Qiagen) that had been equilibrated with buffer A (50 mM NaH_2PO_4, 300 mM NaCl 10 mM imidazole pH 8.0). The column was washed with the same buffer and then eluted stepwise with buffer A containing, 50, 70, 130, 170, and 250 mM imidazole. The polypeptide composition of the column fractions was monitored by SDS-PAGE. The recombinant NS5B protein was retained on the column and recovered in the 130—250 mM imidazole eluate. This fraction was dialyzed against buffer B (25 mM Tris–HCl, pH 7.5, 2.5 mM $MgCl_2$, 1 mM dithiothreitol, 50% glycerol). The protein concentration was determined by the Bio-Rad dye binding method with bovine serum albumin as the standard.

BVDV RNA-Dependent RNA Polymerase Assay: Polymerization was performed in 25-μl reaction volumes. The reaction mixture contained 20 mM Tris, pH 7.5, 20 mM $MnCl_2$, 6 mM $MgCl_2$ 25 mM NaCl, 25% glycerol, 0.5 lg/lL bovine serum albumin, 2 mM dithiothreitol. Our standard reaction used 600 ng of BVDV-NS5B, 100 μM GTP and 300 ng of template poly(rC) preannealed with 25 ng of primer (rG) with or without 50 μM of each inhibitor. Reactions were incubated at 30 °C for 120 min then stopped by addiction of 2 μl of 200 mM EDTA. 175 μl of PicoGreen Quantitation Reagent (Molecular Probes), diluted 1/345 in TE, was added to each sample and incubated at room temperature, protected from ambient light, for 5 min. Fluorescence of samples in wells of a 96-well microtiter plate was determined in a fluorescence microplate reader.

Molecular Modeling All simulations were run on a cluster of Silicon Graphics Octane and performed by using the program packages AutoDock (v. 3.0),[45] AMBER 7.0[46,47] Materials Studio (v.3.2),[48] Discover[49] and in-house developed codes (stand-alone and add-on to the commercial software).

The starting 3-D model of the RdRp was based on its X-ray crystallographic structure (chain B, PBD code: 1CSJ).[50] Water molecules in the coordinate file were removed, and hydrogens were added to the protein backbone and side chains with the PARSE module of the AMBER 6.0 package. All ionizable residues were considered in the standard ionization state at neutral pH. The all-atom force field (FF) parameters by Cornell *et al.*[51] (in *parm94.dat* file of the AMBER 7.0 code) was applied for protein relaxation. The primary cut-off distance for nonbonded interaction was set to 12 Å, the cut-off taper for the Coulomb and van der Waals interactions were 1.2 and 2, respectively. The GB/SA continuum solvation model[57,58] was used to mimic an aqueous environment. Geometry refinement was carried out using the SANDER module *via* a combined steepest descent—conjugate gradient algorithm, using as a convergence criterion for the energy gradient the root-mean-square of the Cartesian elements of the gradient equal to 0.01 kcal/(mol Å). As expected, no relevant structural changes were observed between the active site of the α-CT relaxed structure and the original 3-D structure.

The model structures of all nucleoside analogs considered were generated using the 3-D sketcher tool of Materials Studio. All the molecules were subjected to an initial energy minimization using Discover. In this case, the convergence criterion was set to 10^{-4} kcal/(mol Å). The conformational search was carried out using a combined molecular mechanics/molecular dynamics simulated annealing (MDSA) protocol.[59] Accordingly, the relaxed structures were subjected to 5 repeated temperature cycles (from 25 to 1200 °C and back) using constant volume/constant temperature (NVT) MD conditions. At the end of each annealing cycle, the structures were again energy minimized to converge below 10^{-4} kcal/(mol Å), and only the structures corresponding to the minimum energy were used for further modeling. The electrostatic charges for the geometrically optimized drug molecules were obtained by restrained electrostatic potential fitting,[60] and the electrostatic potentials were produced by single-point quantum mechanical calculations at the Hartree–Fock level with a 6-31G* basis set. All *ab initio* calculations were carried out with *DMol*[3,61] as implemented in the Materials Studio modeling suite.

To proceed with docking simulation, all non-polar hydrogen atoms of the small organic molecules were deleted, and their charges were automatically added to those of the corresponding carbon atom by the program AutoTors included in the suite AutoDock. The relevant grids of affinity potentials used by AutoDock were calculated by running the program AutoGrid. In order to encase a reasonable region of the protein surface and interior volume, centered on the crystallographic identified binding site, the grids were 60 Å on each side. Grid spacing (0.375 Å), and 120 grid points were applied in each Cartesian direction so as to calculate mass-centered grid maps. Amber 12-6 and 12-10 Lennard-Jones parameters were used in modeling van der Waals interactions and hydrogen bonding (N–H, O–H and S–H), respectively. In the generation of the electrostatic grid maps, the distance dependent relative permittivity of Mehler and Solmajer[62] was applied.

For the docking of each drug to the protein, three hundred Monte Carlo/Simulated Annealing (MC/SA) runs were performed, with 100 constant temperature cycles for simulated annealing. Translation, quatern ion parameters, and torsions were set at random before SA runs. Each cycle had a maximum of 20000 accepted or rejected moves, the minimal energy structure being passed to the next cycle. The temperature was reduced by a 0.95 factor per cycle from an initial value of RT = 100 cal/mol. For these calculations, the GB/SA implicit water model was again used to mimic the solvated environment. The rotation of the angles ϕ and φ, and the angles of side chains were set free during the calculations. All other parameters of the MC/SA algorithm were kept as default. Following the docking procedure, all structures of each nucleoside analog were subjected to cluster analysis with a tolerance of 1 Å for an all-atom root-mean-square (RMS) deviation from a lower-energy structure representing each cluster family. The structure with the lowest interaction energy was selected for further evaluation.

Each best drug/RdRp complex resulting from the automated docking procedure was further refined in the AMBER suite using the quenched molecular dynamics method (QMD).[54] In this case, 100 ps MD simulation at 25 °C were employed to sample the conformational space of the inhibitor–enzyme complex in the GB/SA continuum solvation environment.[57] The integration step was equal to 1 fs. After each ps, the system was cooled to −273 °C, the structure was extensively minimized, and stored. To prevent global conformational changes of the enzyme, the backbone of the protein binding site was constrained by a harmonic force constant of 100 kcal/Å, whereas the amino acid side chains and the ligands were allowed to move without any constraint.

For the calculation of the binding free energy in water, the best energy configuration of each complex resulting from the previous step was solvated by a cubic box of TIP3P water molecules[63] extended at least 10 Å in each direction from the solute, and an appropriate number of counter ions were added to neutralize the system. The periodic boundary conditions with constant pressure of 1 atm were applied, and long-range nonbonded van der Waals interactions were truncated by using an 8 Å residue-based cut-off. The particle mesh Ewald method[64] was used to treat the long-range electrostatics. Unfavorable interactions within the structures were relieved with steepest descent followed by conjugate gradient energy minimization until the RMS of the elements in the gradient vector was less than 10^{-4} kcal/(mol Å). Each system was gradually heated to 25 °C in three intervals, allowing a 5 ps interval per each 100 °C, and then equilibrated for 25 ps at 25 °C, followed by 400 ps of data collection runs. The SHAKE algorithm was applied to constrain all bonds to their equilibrium values, thus removing high frequency vibrations.[65] An integration time step of 2 fs has been used with constant temperature, being the temperature maintained at a constant value by the Berendsen coupling algorithm,[66] with separate solute–solvent and

solvent–solvent coupling. A total of 400 snapshots were saved during the data collection period, one snapshot per each 1 ps of MD simulation.

The binding free energy ΔG_{bind} of each complex in water was calculated according to the procedure proposed by Srinivasan *et al.*[55] and will be briefly described below. According to this method, ΔG_{bind} is calculated as:

$$\Delta G_{bind} = \Delta G_{MM} + \Delta G^{C}_{sol} - \Delta G^{L}_{sol} - \Delta G^{P}_{sol} - T\Delta S \quad (1)$$

where ΔG_{MM} is the interaction energy between the ligand and the protein, ΔG^{C}_{sol}, ΔG^{L}_{sol} and ΔG^{P}_{sol} are the solvation free energy for the complex, the ligand and the protein, respectively, and $-T\Delta S$ is the conformational entropy contribution to the binding. All energetic analysis was done for only a single MD trajectory of the drug/protein complex considered, with unbound RdRp and nucleoside analog snapshots taken from the snapshots of that trajectory.

ΔG_{MM} can be obtained from the molecular mechanics (MM) interaction energies as:

$$\Delta G_{MM} = \Delta G^{ele}_{int} + \Delta G^{vdW}_{int} \quad (2)$$

where ΔG^{ele}_{int} and ΔG^{vdW}_{int} are the electrostatic and van der Waals contributions to the interaction energy between the ligand and the receptor. We must point out here that the molecular mechanics energy ΔG_{MM} in Eq. 2 effectively consists also of a valence part, ΔG^{val}_{int}, but, since the structure of the protein in its bound and unbound state is the same, the contribution of this term to the binding free energy is zero. Accordingly, its term has been omitted in Eq. 2. In our case, these quantities were calculated with the *anal* and *carnal* modules from the AMBER 7.0 suite. The infinite cutoffs for all interactions and the *parm94* force field parameters[51] were applied. The total solvation energy, ΔG_{sol}, is divided in two parts: the electrostatic contribution, ΔG^{ele}_{sol}, and the non-polar term, ΔG^{np}_{sol}:

$$\Delta G_{sol} = \Delta G^{ele}_{sol} + \Delta G^{np}_{sol} \quad (3)$$

The polar component of ΔG_{sol} was evaluated with the PB approach.[67] This procedure involves using a continuum solvent model, which represents the solute as a low dielectric medium (*i.e.* of dielectric constant $\varepsilon=1$) with embedded charges and the solvent as a high dielectric medium ($\varepsilon=80$) with no salt. All atomic charges were taken from the Cornell *et al.* force field,[51] since these are consistent with the MM energy calculations. However, as suggested by Chong *et al.*,[68] the atomic radii were taken from the PARSE parameter set[69] instead of the *parm94* FF set because of the small size of hydrogens in the latter. The dielectric boundary is the contact surface between the radii of the solute and the radius (1.4 Å) of a water molecule. The numerical solution of the linearized Poisson–Boltzmann equations were solved on a cubic lattice by using the iterative finite-difference method implemented in the *DelPhi* software package.[70] The grid size used was 0.5 Å. Potentials at the boundaries of the finite-difference lattice were set to the sum of the Debye–Hückel potentials.

The non polar contribution to the solvation energy ΔG^{np}_{sol} was calculated from the following empirical equation:

$$\Delta G^{np}_{sol} = \gamma SA + b \quad (4)$$

in which $\gamma=0.00542$ kcal/Å^2, $b=0.92$ kcal/mol, and SA is the solvent-accessible surface estimated with the MSMS[71] program.

To complete the estimate of the free energy of binding, we should also calculate the entropy components arising from the solute degrees of freedom. Accordingly, the normal-mode analysis approach was followed to estimate the last parameter, *i.e.* the change in solute entropy upon association $-T\Delta S$.[72]

Acknowledgements This work was supported by Ministero della Istruzione Università e Ricerca: FIRB2001 RBNE01J3SK_009, FIRB2001–RBNE01J3SK_006 and FIRB2001–RBNE01J3SK_001. We thank Paul Leeson for the careful revision of English language.

References and Notes

1) Leyssen P., De Clerck E., Neyts J., *Clin. Microbiol. Rev.*, **13**, 67—82 (2000).
2) Francki R. I., Fauquet D. L., Knudson D. L., Brown F., *Arch. Virol.*, **2** (Suppl.), 223—233 (1991).
3) Hougthon M., "Hepatitis C viruses. In Field Virology," 3rd ed., ed. by Field B. N., Knipe D. M., Howley P. M., Lippincott-Raven, Philadelphia, 1996, pp. 1035—1058.
4) Monath T. P., Heinz F. X., "Flavivirus. In Field Virology," 3rd ed., ed. by Field B. N., Knipe D. M., Howley P. M., Lippincott-Raven, Philadelphia, 1996, pp. 961—1034.
5) Thiel H. J., Plagemann P. G. W., Moenning V., "Pestivirus. In Field Virology," 3rd ed., ed. by Field B. N., Knipe D. M., Howley P. M., Lippincott-Raven, Philadelphia, 1996, pp. 1059—1073.
6) Van Oirschot J. T., Bruschke C. J., van Rijn P. A., *Vet. Microbiol.*, **64**, 169—183 (1999).
7) Baginski S. G., Pevear D. C., Seipel M., Sun S. C. C., Benetatos C. A., Chunduru S. K., Rice C. M., Collett M. S., *Proc. Natl. Acad. Sci. U.S.A.*, **97**, 7981—7986 (2000).
8) King R. W., Scarnati H. T., Priestley E. S., De Lucca I., Bansal A., Williams J. K., *Antiviral Chem. Chemother.*, **13**, 315—323 (2002).
9) Sun J. H., Lemm J. A., O'Boyle D. R., II, Racela J., Colonno R., Gao M., *J. Virol.*, **77**, 6753—6760 (2003).
10) Bukhtiyarova M., Rizzo C. J., Kettner C. A., Korant B. D., Scarnati H. T., King R. W., *Antiviral Chem. Chemother.*, **12**, 367—373 (2002).
11) Givens M. D., Dykstra C. C., Brock K. V., Stringfellow D. A., Kumar A., Stephens C. E., Goker H., Boykin D. W., *Antimicrob. Agents Chemother.*, **47**, 2223—2230 (2003).
12) Branza-Nichita N., Durantel D., Carrouée-Durantel S., Dwek R. A., Zitzmann N., *J. Virol.*, **75**, 3527—3536 (2001).
13) Durantel D., Branza-Nichita N., Carrouée-Durantel S., Butters T. D., Dwek R. A., Zitzmann N., *J. Virol.*, **75**, 8987—8998 (2001).
14) Zitzmann N., Mehta A. S., Carrouée S., Butters T. D., Platt F. M., McCauley J., Blumberg B. S., Dwek R. A., Block T. M., *Proc. Natl. Acad. Sci. U.S.A.*, **96**, 11878—11882 (1999).
15) Markland W., McQuaid T. J., Jain J., Kwong A. D., *Antimicrob. Agents Chemother.*, **44**, 859—866 (2000).
16) Paeshuyse J., Leyssen P., Mabery E., Boddeker N., Vrancken R., Froeyen M., Ansari I. H., Dutartre H., Rozenski J., Gil L. H. V. G., Letellier C., Lanford R., Canard B., Koenen F., Kerkhofs P., Donis R. O., Herdewijn P., Watson J., De Clercq E., Puerstinger G., Neyts J., *J. Virol.*, **80**, 149—160 (2006).
17) Blight K. J., Grakoui A., Hanson H. L., Rice C. M., "The molecular biology of hepatitis C virus. In Hepatitis Viruses," ed. by Ou J. H. J., Kluwer Academic, Boston, 2002, pp. 81—108.
18) Kim W. R., Brown R. S., Jr., Terrault N. A., El-Serag H., *Hepatology*, **36**, 227—242 (2002).
19) Tan S. L., Pause A., Shi Y., Sonenberg N., *Nat. Rev. Drug Discov.*, **1**, 867—881 (2002).
20) Buckwold V. E., Beer B. E., Donis R. O., *Antiviral Res.*, **60**, 1—15 (2003).
21) Bartenschlager R., Lohmann V., *Antiviral Res.*, **52**, 1—17 (2001).
22) Bartenschlager R., *Nat. Rev. Drug Discov.*, **1**, 911—916 (2002).
23) Manfredini S., Baraldi P. G., Durini E., Vertuani S., Balzarini J., De Clercq E., Karlsson A., Buzzoni V., Thelander L., *J. Med. Chem.*, **42**, 3243—3250 (1999).
24) Manfredini S., Baraldi P. G., Bazzanini R., Marangoni M., Simoni D., Balzarini J., De Clercq E., *J. Med. Chem.*, **38**, 199—203 (1995).
25) Manfredini S., Angusti A., Veronese A. C., Durini E., Vertuani S., Nalin F., Solaroli N., Pricl S., Ferrone M., Mura M., Musiu C., Piano M. A., Poddesu B., Marturana F., La Colla P., *Pure Appl. Chem.*, **76**, 1007—1015 (2004).
26) Nair V., Chamberlain S. D., *J. Org. Chem.*, **50**, 5069—5075 (1985).
27) Ogilvie K. K., Beaucage S. L., Schifman A. L., Theriault N. Y., Sadana K. L., *Can. J. Chem.*, **56**, 2768—2780 (1978).
28) Ogilvie K. K., Hakimelahi G. H., Proba Z. A., McGee D. P., *Tetrahedron Lett.*, **23**, 1997—2000 (1982).
29) Beaton G., Jones A. S., Walker R. T., *Tetrahedron*, **44**, 6419—6431 (1988).
30) Barton D. H. R., Jang D. O., Jaszberenyi J. C., *Tetrahedron*, **49**, 7193—7214 (1993).
31) Watkins B. E., Kiely J. S., Rapoport H., *J. Am. Chem. Soc.*, **104**, 5702—5708 (1982).
32) Hansske F., Madej D., Robins M. J., *Tetrahedron*, **40**, 125—135 (1984).
33) Baker D. C., Kumar S. D., Waites W. J., Arnett G., Shannon W. M., Higuchi W. I., Lambert W. J., *J. Med. Chem.*, **27**, 270—274 (1984).
34) Erion M. D., Reddy K. R., Boyer S. H., Matelich M. C., Gomez-Galeno J., Lemus R. H., Ugarkar B. G., Colby T. J., Schanzer J., Poelje P. D., *J. Am. Chem. Soc.*, **126**, 5154—5163 (2004).
35) Henke C., Pfleiderer W., *Nucleos. Nucleot. Nucl.*, **24**, 1665—1706 (2005).
36) Gmeiner W. H., Pon R. T., Lown J. W., *J. Org. Chem.*, **56**, 3602—3608 (1991).

37) Golisade A., Van Calenbergh S., Link A., *Tetrahedron*, **56**, 3167—3172 (2000).
38) Robins M. J., Wilson J. S., Hansske F., *J. Am. Chem. Soc.*, **105**, 4059—4065 (1983).
39) Maguire A. R., Meng W. D., Roberts S. M., Willetts A. J., *J. Chem. Soc., Perkin Trans. 1*, **15**, 1795—1808 (1993).
40) Kupche, E. L., *Chem. Nat. Compd.* (Engl. Transl.), **18**, 327—331 (1982).
41) Takamura T., Kato T., Arakawa E., Ogawa S., Suzumura Y., Kato T., *Chem. Pharm. Bull.*, **37**, 2828—2831 (1989).
42) Thomas H. J., Montgomery J. A., *J. Org. Chem.*, **31**, 1413—1416 (1966).
43) Kawasaki A. M., Casper M. D., Freier S. M., Lesnik E. A., Zounes M. C., Cummins L. L., Gonzalez C., Cook P. D., *J. Med. Chem.*, **36**, 831—841 (1993).
44) Mosmann T., *S. Immunol. Methods*, **65**, 55—63 (1983).
45) Morris G. M., Goodsell D. S., Halliday R. S., Huey R., Hart W. E., Belew R. K., Olson A. J., *J. Comput. Chem.*, **19**, 1639—1662 (1998).
46) Case D. A., Pearlman D. A., Caldwell J. W., Cheatham III T. E., Wang J., Ross W. S., Simmerling C. L., Darden T. A., Merz K. M., Stanton R. V., Cheng A. L., Vincent J. J., Crowley M., Tsui V., Gohlke H., Radmer R. J., Duan Y., Pitera J., Massova I., Seibel G. L., Singh U. C., Weiner P. K., Kollman P. A., "AMBER 7 2002," University of California, San Francisco, CA, U.S.A.
47) Pearlman D. A., Case D. A., Caldwell J. W., Ross W. S., Cheatham III T. E., DeBolt S., Ferguson D., Seibel G. L., Kollman P. A., *Comp. Phys. Commun.*, **91**, 1—41 (1995).
48) Materials Studio Program Package (v. 3.2), Accelrys Inc., San Diego, CA, U.S.A.
49) Discover Program Package, Accelrys Inc. San Diego, CA, U.S.A.
50) Bressanelli S., Tomei L., Roussel A., Incitti I., Vitale R. L., Mathieu M., De Francesco R., Rey F. A., *Proc. Natl. Acad. Sci. U.S.A.*, **96**, 13034—13039 (1999).
51) Cornell W. D., Cieplak P., Bayly C. I., Gould I. R., Merz K. M., Ferguson D. M., Spellmeyer D. C., Fox T., Caldwell J. W., Kollman P. A., *J. Am. Chem. Soc.*, **117**, 5179—5197 (1995).
52) Felluga F., Pitacco G., Valentin E., Coslanich A., Fermeglia M., Ferrone M., Pricl S., *Tetrahedron: Asymmetry*, **14**, 3385—3399 (2003).
53) Mamolo M. G., Zampieri D., Vio L., Fermeglia M., Ferrone M., Pricl S., Scialino G., Banfi E., *Bioorg. Med. Chem.*, **13**, 3797—3809 (2005).
54) Frecer V., Kabelac M., De Nardi P., Pricl S., Miertus S., *J. Mol. Graphics Modell.*, **22**, 209—220 (2004).
55) Srinivasan J., Cheatham T. E., Cieplak P., Kollman P. A., Case D. A., *J. Am. Chem. Soc.*, **120**, 9401—9409 (1998).
56) Showell G. A., Mills J. S., *Drug. Discov. Today*, **15**, 551—556 (2003).
57) Jayaram B., Sprous D., Beveridge D. L., *J. Phys. Chem. B*, **102**, 9571—9576 (1998).
58) Weiser J., Shenkin P. S., Still W. C., *J. Comp. Chem.*, **20**, 217—230 (1999).
59) Metullio L., Ferrone M., Coslanich A., Fuchs S., Fermeglia M., Paneni M. S., Pricl S., *Biomacromolecules*, **5**, 1371—1378 (2004).
60) Bayly C. I., Cieplak P., Cornell W. D., Kollman P. A., *J. Phys. Chem.*, **97**, 10269—10280 (1993).
61) Delley B., *J. Chem. Phys.*, **92**, 508—520 (1990).
62) Mehler E. L., Solmajer T., *Protein Engng.*, **4**, 903—910 (1991).
63) Jorgensen W. L., Chandrasekhar J., Madura J. D., Impey R. W., Klein M. L., *J. Chem. Phys.*, **79**, 926—935 (1983).
64) Darden T., York D., Pedersen L., *J. Chem. Phys.*, **98**, 10089—10092 (1993).
65) Ryckaert J. P., Ciccotti G., Berendsen H. J. C., *J. Comput. Phys.*, **23**, 327—341 (1977).
66) Berendsen H. J. C., Postma J. P. M., vanGunsteren W. F., DiNola A., Haak J. R., *J. Chem. Phys.*, **81**, 3684—3690 (1984).
67) Sharp K. A., Honig B. H., *Annu. Rev. Biophys. Chem.*, **19**, 301—312 (1990).
68) Chong L. T., Duan Y., Wang L., Massova I., Kollman P. A., *Proc. Natl. Acad. Sci. U.S.A.*, **96**, 14330—14335 (1999).
69) Sitkoff D., Sharp K. A., Honig B. H., *J. Phys. Chem.*, **98**, 1978—1988 (1994).
70) Gilson M. K., Sharp K. A., Honig B. H., *J. Comput. Chem.*, **9**, 327—335 (1988).
71) Sanner M. F., Olson A. J., Spehner J. C., *Biopolymers*, **38**, 305—320 (1996).
72) Wilson E. B., Decius J. C., Cross P. C., "Molecular Vibrations," McGraw-Hill, New York, 1995.